**Atmospheric
Measurement
Techniques**

A liquid nitrogen-free preconcentration unit for measurements of ambient N_2O isotopomers by QCLAS

J. Mohn[1], C. Guggenheim[1], B. Tuzson[1], M. K. Vollmer[1], S. Toyoda[2], N. Yoshida[2], and L. Emmenegger[1]

[1]Laboratory for Air Pollution & Environmental Technology, EMPA, Dübendorf, Switzerland
[2]Department of Environmental Chemistry and Engineering, Tokyo Institute of Technology, Yokohama, Japan

Abstract. Important information about the biogeochemical cycle of nitrous oxide (N_2O) can be obtained by measuring its three main isotopic species, $^{14}N^{15}N^{16}O$, $^{15}N^{14}N^{16}O$, and $^{14}N^{14}N^{16}O$, and the respective site-specific relative isotope ratio differences $\delta^{15}N^{\alpha}$ and $\delta^{15}N^{\beta}$. Absorption laser spectroscopy in the mid-infrared is a direct method for the analysis of the ^{15}N isotopic composition of N_2O, yet not sensitive enough for atmospheric N_2O mixing ratios (320 ppb). To enable a fully-automated high precision analysis of N_2O isotopic species at ambient mixing ratios, we built and optimized a liquid nitrogen-free preconcentration unit to be coupled to a quantum cascade laser (QCL) based spectrometer. During standard operation 10 l of ambient air are preconcentrated on a HayeSep D trap and desorbed in 50 ml of synthetic air. Rigorous tests were conducted, using FTIR, quantum cascade laser absorption spectroscopy (QCLAS), GC-FID and component-specific ozone and oxygen analysers to investigate recovery rates, conservation of isotopic signatures and spectral interferences after preconcentration. We achieve quantitative N_2O recovery of >99% with only minor, statistically not significant isotopic fractionation and no relevant spectral interferences from other atmospheric constituents. The developed preconcentration unit also has the potential to be applied to other trace gases and their isotopic composition.

1 Introduction

Nitrous oxide (N_2O) is currently the most important anthropogenic ozone depleting substance and exerts the second largest global warming potential weighted (GWP) emission of non-CO_2 greenhouse gases (Ravishankara et al., 2009).

Since pre-industrial times, N_2O mixing ratios in the troposphere increased from 270 ppb (parts-per-billion, 10^{-9} moles of trace gas per mole of dry air) to the current level of 320 ppb at a rate of 0.26% a^{-1}. The predominant sources of N_2O on a global scale are microbial production in agricultural and natural soils as well as rivers, estuaries, coastal areas and oceans. While the major sink, stratospheric destruction, is well quantified, the strengths of individual N_2O sources remain largely uncertain (Solomon et al., 2007).

Important information about the biogeochemical cycle of N_2O can be obtained by measuring the intramolecular distribution of ^{15}N in atmospheric N_2O (Billings, 2008; Bernard et al., 2006; Ishijima et al., 2007; Rahn and Wahlen, 2000; Röckmann et al., 2003; Röckmann and Levin, 2005; Yoshida and Toyoda, 2000). N_2O is a linear tri-atomic molecule with one nitrogen atom in the centre (2 or α site) and one at the end (1 or β site) that leads to four possible stable isotopic species with respect to nitrogen isotopes. The most abundant N_2O isotopic species in the atmosphere are $^{14}N^{14}N^{16}O$ (99%), $^{15}N^{14}N^{16}O$ (0.37%) and $^{14}N^{15}N^{16}O$ (0.37%) (Werner and Brand, 2001; Yoshida and Toyoda, 2000). Isotope abundances are usually reported in the δ-notation, where $\delta^{15}N$ denotes the relative difference in ‰ of the $^{15}N/^{14}N$ ratio of the sample versus the reference material (atmospheric N_2), analogically $\delta^{15}N^{\beta}$ denotes the corresponding ratio for $^{15}N^{14}N^{16}O$ vs. $^{14}N^{14}N^{16}O$.

The bulk nitrogen δ value ($\delta^{15}N^{\text{bulk}}=(\delta^{15}N^{\alpha}+\delta^{15}N^{\beta})/2$) tropospheric N_2O was found to be enriched by 6.3±0.3‰ to 6.72 ± 0.12‰ relative to air-N_2 (Yoshida and Toyoda, 2000; Toyoda et al., 2004; Kaiser et al., 2003; Park et al., 2004), with a strong site preference (SP=$\delta^{15}N^{\alpha}-\delta^{15}N^{\beta}$) of 18.7±2.2‰ for the central nitrogen atom (Yoshida and Toyoda, 2000). Tropospheric N_2O mixing ratios and isotopic composition are largely controlled by back injection of stratospheric N_2O as well as N_2O emissions from microbial activity and combustion processes. In the stratosphere, the abundance of the heavier isotopologues and the SP increases

with altitude to values as high as 140‰ for $\delta^{15}N^{bulk}$ (Kaiser et al., 2006) and 100‰ for SP (Toyoda et al., 2001), mainly due to isotopic fractionation during UV-induced photolysis and oxidation. Isotopic signatures of different N_2O emission sources were found to vary largely between approx. -50‰ (soil) to 10‰ (coal combustion) for $\delta^{15}N^{bulk}$ and -5‰ (soil) to 35‰ (ocean) for the SP (Toyoda et al., 2009, and references therein). An overview on atmospheric applications of N_2O isotopic analysis can be found in a review publication of Brenninkmeijer et al. (2003). The required analytical precision for $\delta^{15}N^{\alpha}$ and $\delta^{15}N^{\beta}$ depends strongly on the application and may vary between < 0.1‰ for firn air analysis to 1‰ for subsoil N_2O studies.

Currently, the only technique for N_2O isotopic measurements at ambient mixing ratios is laboratory-based isotope-ratio mass-spectrometry (IRMS) in combination with flask-sampling and cryogenic preconcentration. However, isotopomers such as $^{14}N^{15}N^{16}O$ and $^{15}N^{14}N^{16}O$ cannot be distinguished directly by IRMS, as they have the same mass. To determine the site-selective isotopic composition, the ^{15}N content of the NO^+ and N_2O^+ fragment and molecule ions of N_2O has to be analyzed (Brenninkmeijer and Röckmann, 1999; Toyoda and Yoshida, 1999). Therefore, the masses m/z 44, 45, and 46 (for N_2O) and m/z 30 and 31 (for NO) are monitored either simultaneously (on last generation IRMS) or after two separate sample injections. Although IRMS is a well-known method with excellent precision (0.05‰–0.9‰) and accuracy (Röckmann and Levin, 2005; Well et al., 2008; Yoshida and Toyoda, 2000), it has some disadvantages such as the large size of the instrument, which hinders field measurements. The required field sampling and sample storage strongly limits its use for the characterization of variations in N_2O isotopic species at time-scales relevant to many environmental processes.

Laser spectroscopy is a valuable alternative, because compact and continuously-operating instruments can be developed that allow for extended field measurements. This offers the possibility for process studies and opens a completely new field of applications. Furthermore, the method is inherently selective, even for molecules with the same mass, because it is based on the highly characteristic rotational-vibrational transitions of the different N_2O isotopic species. The absorption lines of the various species can be easily resolved at low cell pressure. However, there are only a few spectroscopic measurements on isotope ratios of N_2O, and these were performed on pure N_2O samples (Gagliardi et al., 2005; Nakayama et al., 2007; Uehara et al., 2001, 2003) with the exception of two recent studies (Wächter et al., 2008; Wächter and Sigrist, 2007). The reported precisions range between 0.2‰ and 9‰.

Recent advances in laser technology provided a new class of mid-infrared (IR) semiconductor lasers: the unipolar intersubband quantum cascade lasers (QCL). They have the advantage of operating at non-cryogenic temperatures (quasi room-temperature) with high spectral purity and relatively high power output (Faist et al., 1994). The application of these light sources for high-precision isotope ratio measurement has been recently demonstrated for CO_2 by Nelson et al. (2008) and Tuzson et al. (2008a, b). Spectroscopy in the mid-IR region is particularly effective for molecules that exhibit strong fundamental vibrations, such as CO_2 and N_2O, with line intensities about two orders of magnitude higher than in the near-IR. We recently demonstrated a precision of 0.5‰ for $\delta^{15}N$ at N_2O mixing ratios of 90 ppm (Wächter et al., 2008) using a pulsed QCL emitting at 4.6 µm. Atmospheric N_2O mixing ratios (320 ppb), however, are more than two orders of magnitude lower and are therefore currently not accessible for direct isotopic analysis by laser spectroscopy.

For these reasons we suggest to combine laser spectroscopy with preconcentration techniques to increase N_2O mixing ratios from ambient levels to ≈60 ppm. The developed custom-built preconcentration unit enables us to make use of the precision and site specificity of QCLAS at a temporal resolution of approx. 30 min. The preconcentration technique we employ is fully automated and is based on a commercial closed-loop cryogenic unit and thereby free of consumables like liquid nitrogen. Here we describe the most important properties that were obtained through systematic optimization and characterization: (a) excellent recovery of N_2O and other trace gases; (b) conservation of the N_2O isotopic composition, and (c) negligible impact of other atmospheric constituents (e.g. CO_2, H_2O, CO, O_3, CH_4 and C_2H_2) on the analyzed N_2O isotope ratios. Our results also indicate that the coupling of preconcentration and laser spectroscopy may also be feasible for the measurement of mixing ratios and isotopic composition of other trace gases (e.g. many VOCs, CH_4, CO).

2 Experimental

2.1 Instrumental

2.1.1 Preconcentration unit

The technology of our preconcentration unit is based on a previously developed system called "Medusa" which was originally designed for halogenated compounds measurements by gas-chromatography mass-spectrometry (Miller et al., 2008). We re-designed and optimized the system for the preconcentration of N_2O isotopic species and their subsequent quantification by laser spectroscopy. One main reason to choose this system is the combination of a relatively mild adsorbent trap with a low-temperature refrigeration unit reaching $<-150\,°C$. Our preconcentration unit differs from "Medusa" by a number of key elements, including: an optimized setup with two multiport valves and a low temperature adsorbent trap. Furthermore, all gas flows are significantly increased and regulated by mass flow controllers (MFC,
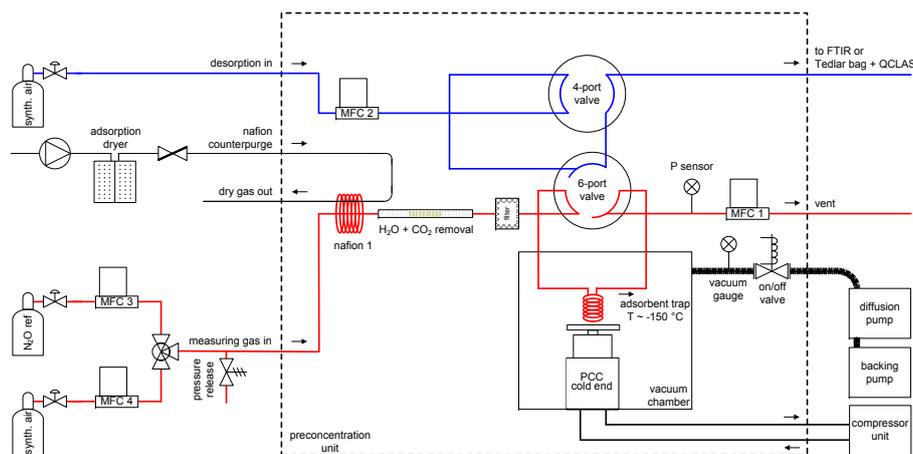
Fig. 1. Process chart during trap loading (phase II) with N_2O in synthetic air.

Redy Smart Series, Vögtlin Instruments, Switzerland) and the complete preconcentration unit is controlled and monitored by LabVIEW (National Instruments Corp., USA).

The instrument flow scheme is illustrated in Fig. 1, showing one particular position of the valves (Valco Instruments Inc, Switzerland), which are used to isolate or combine various sections of the sample pathways. The 6-port valve is equipped with an elongated-groove rotor and driven by a multi-position actuator which enables more than 2 valve positions. Rotating the 4-port valve will change the flow direction through the HayeSep D trap. The preconcentration trap consists of stainless steel tubing (ID 1.6 mm, OD 2.1 mm) filled with 200 mg HayeSep D (100–120 mesh, Hayes Separations Inc., USA) and coiled onto an aluminium tube standoff. The standoff is attached to a copper base-plate cooled by the refrigeration unit (PCC: Polycold Compact Cooler, Brooks Automation, USA), and located in a vacuum chamber. The trap reaches temperatures of $\approx -150\,°C$ and can be heated resistively to $> 100\,°C$, using a custom-built trap heating unit coupled with an Omega PID controller (CN77354-C2, Omega Engineering Inc., USA).

The operation sequence and parameter settings (e.g. flow rates, temperatures and timing) of the preconcentration unit were optimized to obtain a sharp N_2O concentration profile during desorption. The principle of operation is described in the following paragraphs (see Figs. 1 and 2): after an initialization phase that sets all parameters to their starting values, the HayeSep D trap is purged by back-flushing with 50 sccm (standard cubic centimetre per minute) of high purity synthetic air and heated to approx. $100\,°C$ (phase I). This phase assures the absence of residual trace gases on the preconcentration trap and reproducible starting conditions. After cooling the trap down to $\approx -150\,°C$, the loading (phase II) is initialized by setting the sample gas flow to 500 sccm, flushing the lines and rotating the 6-port valve to the loading position. H_2O and CO_2 are removed from the measuring gas
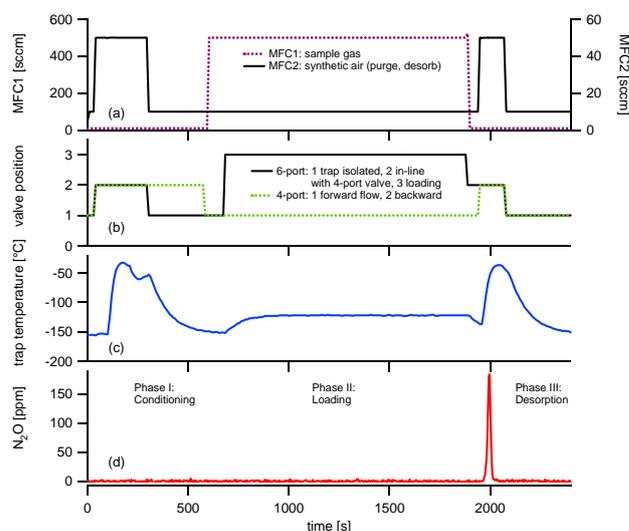
Fig. 2. Typical N_2O adsorption/desorption process (adsorption of 500 sccm of 350 ppb N_2O in synthetic air; 10 l sample volume) with preceding trap conditioning: **(a)** sample gas flow (MFC1) and flow of synthetic air (MFC2); **(b)** position of 6-port and 4-port valves; **(c)** trap temperature; **(d)** N_2O mixing ratios as analyzed by on-line FTIR spectroscopy.

by a Nafion^{TM} drier (MD-050-72S-1, PermaPure Inc., USA) and a chemical trap filled with Ascarite (3 g, 10–35 mesh, Fluka, Switzerland) bracketed by $Mg(ClO_4)_2$ (2·3 g, Fluka, Switzerland). To purge residual gas molecules onto the trap, a short post-flush with synthetic air is applied at the end of phase II. Rotating the 4-port valve to position 2 (backward flow) and adjusting the flow of synthetic air to 50 sccm initiates desorption (phase III). After setting the trap temperature to $-35\,°C$, an immediate release of N_2O (boiling point $-88.5\,°C$) can be observed by FTIR spectroscopy (see

Fig. 2). Finally, all parameters and conditions are set back to their initial values. The duration of trap loading (phase II) and desorption (phase III) are adjusted based on the desired/available sample volume (standard procedure: 20 min at 500 sccm sampling flow results in 10 l sample volume) and the desired N_2O output mixing ratio, usually around 60 ppm for high precision N_2O isotopic analysis by QCLAS. The minimal desorption time for quantitative N_2O recovery depends on the molar N_2O input and was determined by on-line FTIR spectroscopy to be between 60 s for 140 nmol and 180 s for 4000 nmol N_2O. Typically a 10 l ambient air sample is focused into 50 ml desorption volume, corresponding to a concentration factor of 200.

2.1.2 On-line FTIR analysis of mixing ratios

We employed a Nicolet Avatar 370 MCT spectrometer (Thermo Nicolet Corp., USA) equipped with a heated (40 °C) low-volume (50 ml) flow-through gas cell with 1 m pathlength (Model LFT-210, Axiom Analytical Inc., USA). An infrared spectrum with $0.5 \, cm^{-1}$ optical resolution was recorded every three seconds, and trace gas (N_2O, CO, CH_4, CO_2 and H_2O) mixing ratios were retrieved by classical least square fitting in selected wavelength regions (Mohn et al., 2004, 2008). Calibration spectra were recorded under identical instrumental and spectroscopic conditions from certified and diluted calibration gases or by continuous injection of liquids into nitrogen. The detection limits (VDI, 1995) for the trace gases in the undiluted gas were: 100 ppb N_2O, 200 ppb CH_4, 1 ppm CO_2, 200 ppb CO, 10 ppm H_2O. The expanded standard uncertainty for these components is around 10% (95% confidence level). The response time (t_{95}) for the experimental setup (sampling line, FTIR gas cell) was 55 s at the applied flow rate of 50 sccm and 13 s employing a fed-in flow of 450 sccm synthetic air in front of the gas cell to determine the minimal desorption time of the preconcentration unit.

2.1.3 Analysis of the ^{15}N isotopic composition of N_2O by QCLAS

The QCL based spectrometer used in the present project is an improved version of the instrument used by Wächter et al. (2008). The experimental setup consists of a single-mode, pulsed quantum cascade laser emitting at 4.6 µm, a multipass absorption cell (optical path length 56 m, volume 500 ml; Aerodyne Research Inc., USA) and a detection system with pulse normalization. Laser control, data acquisition and real-time signal processing are performed by the TDLWintel software (Aerodyne Research Inc., USA). The main upgrades include: (a) a new RT-QCL (Alpes Lasers SA, Switzerland) with about 10 times more power and a considerably narrower line width of $0.0068 \, cm^{-1}$; (b) a new generation thermo-electrically cooled detector (PVI-3TE-5, Vigo System, PL) with a specific detectivity (D*) $> 10^{11} \, cm \, Hz^{1/2} \, W^{-1}$ at 4.5–
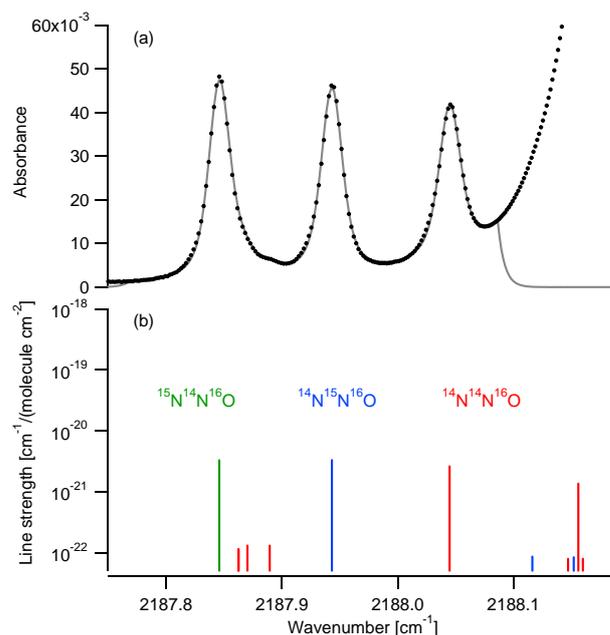
Fig. 3. (a) Measured (dots) and fitted spectrum (solid line) of the N_2O isotopic species at 90 ppm and **(b)** the corresponding line strengths. The tail of a strong absorption line of $^{14}N^{14}N^{16}O$ ($2188.19 \, cm^{-1}$) is clearly visible and was considered in the fit up to $2188.1 \, cm^{-1}$.

4.6 µm, coupled to a miniaturized preamplifier and TEC-controller (MTCC-01, Vigo System, PL). The detector assembly is mounted on a water-cooled cold-plate, which maintains a stable heat-sink temperature of 15±0.1 °C. Further improvements were achieved by redesigning the laser current and temperature control unit, optimizing the laser pulser electronics and the 3-D-alignment stage of the collimating optics for a better alignment stability. The selected absorption lines for this study are shown in Fig. 3. They are located within the scanning range of the laser and have sufficiently strong line strength with similar absorbance for each isotopic species. Mixing ratios for the different species are obtained by simultaneously fitting a low-order polynomial to the spectral baseline and a Gaussian-convoluted Voigt profile to the observed absorption lines, taking into account the measured path length, gas temperature (∼307 K), pressure (8 kPa) and laser line width. For the site-specific relative isotope ratio differences $\delta^{15}N^{\alpha}$ and $\delta^{15}N^{\beta}$, a precision of 0.2–0.3‰ was obtained at 90 ppm N_2O using the Allan variance approach (Werle et al., 1993, data not shown). Analysis of N_2O mixing ratios (Sect. 2.2.1) was performed at $2188.19 \, cm^{-1}$. The QCL spectrometer was operated with a continuous input gas flow of 50–70 sccm.

Table 1. Trace gas mixing ratios and N_2O isotopic composition.

	N_2O [ppm]	$\delta^{15}N^{\alpha}$ [‰]	$\delta^{15}N^{\beta}$ [‰]	CO_2 [ppm]	CH_4 [ppm]	CO [ppb]	O_3 [ppb]	H_2O [ppm]
trace gas recovery [a]	0.39	n.a.	n.a.	35	2.0	350	–	25
	0.35	n.a.	n.a.	–	–	–	–	–
	0.90	n.a.	n.a.	–	–	–	–	–
	9.0	n.a.	n.a.	–	–	–	–	–
isotopic fractionation [b]	0.35	+25.9	+25.2	–	–	–	–	–
	0.90	+25.9	+25.2	–	–	–	–	–
	9.0	+25.9	+25.2	–	–	–	–	–
spectral interference [c]	0.35	n.a.	n.a.	400	2.0	200–450	62–65	1–2%

n.a.: not analyzed
[a] gas mixtures prepared from 9 or 90 ppm N_2O reference gas and synthetic air;
line 1: additionally with pressurized air and mixing ratios determined by FTIR.
[b] gas mixtures prepared from a 90.8 ppm N_2O reference gas analysed by IRMS.
[c] ambient air; N_2O and CO_2 mixing ratios based on estimates, all other mixing ratios taken
from routine measurements of the Swiss National Air Pollution Monitoring Network (NABEL).

2.2 Validation of N_2O preconcentration unit

To validate the N_2O preconcentration unit, tests were performed on the quantitative recovery of N_2O and other trace gases (Sect. 2.2.1), on the conservation of the N_2O δ values ($\Delta\delta^{15}N=\delta^{15}N_{precon}-\delta^{15}N_{original}$) (Sect. 2.2.2), and on the composition of preconcentrated ambient air and its potential interferences with N_2O isotopic analysis (Sect. 2.2.3).

To investigate the trace gas recoveries and isotopic fractionation effects, gas mixtures with known mixing ratios and/or isotopic composition were prepared from standard reference gases by dynamic dilution with high purity synthetic air (79.5% N_2 purity 5.0, 20.5% O_2 purity 5.0, $N_2O <$ 0.3 ppb) and/or pressurized air using a pair of MFCs. Standard reference gases applied include 9.0 ppm and 90 ppm N_2O in synthetic air (Messer Schweiz, Switzerland) to determine the trace gas recoveries and gravimetrically prepared 90.8 ppm N_2O in synthetic air (Wächter et al., 2008) with a distinct isotopic composition of $\delta^{15}N^{\alpha}=25.9\pm0.4$‰ and $\delta^{15}N^{\beta}=25.2\pm1.0$‰ as analysed by IRMS (Toyoda and Yoshida, 1999) to investigate the conservation of the N_2O δ values. Table 1 summarizes the gas mixtures used during the various validation experiments. For the study of spectral interference we relied on ambient air sampled with a membrane pump (PTFE coated membrane, N 035 AT.18, KNF Neuberger, Switzerland).

2.2.1 Trace gas recovery

For the determination of the trace gas recovery, 1 to 10 l of a gas mixture were supplied at a flow rate of 100 sccm, containing N_2O, CH_4 and CO at ambient and H_2O and CO_2 at sub-ambient mixing ratios (Table 1). While these tests were based on the standard preconcentration procedure, no chemical trap was employed to investigate the influence of H_2O and CO_2 traces on the N_2O adsorption. On-line FTIR measurements were performed to obtain time-resolved information on the trace gas mixing ratios desorbed from the HayeSep D trap. The amount of desorbed trace gases was calculated as the integral over time of the output trace gas mixing ratio and the flow rate of synthetic air applied for desorption. The chosen approach has the advantage of analyzing the recovery for different trace gases under standard operation conditions but does not allow a highly precise budgeting because it relies on a fast integration over a wide range of mixing ratios and on MFCs and gas flows that are different during adsorption and desorption.

To achieve an even better precision for the determination of the N_2O recovery, a second approach was used. These further experiments were designed to yield the same mixing ratio before and after the preconcentration step due to the use of the same MFC (MFC2) and flow parameters (2400 s and 100 sccm) during adsorption and desorption, and by collecting the desorbed sample in a 10 l Tedlar bag (Product No. 245-08, SKC Inc., USA). The sample gas was dynamically diluted from a tank, containing either 9.0 or 90 ppm N_2O in synthetic air, with synthetic air to ambient (350 ppb), intermediate (900 ppb) or process (9.0 ppm) mixing ratios (Table 1). N_2O mixing ratios in the sample gas and in the desorbed sample (Tedlar bag) were compared based on QCLAS at 2188.19 cm^{-1}. Experiments at every mixing ratio were replicated thrice. Small differences ($<$1%) between the adsorbed and desorbed gas volumes, as recorded from the MFC output, were corrected.

2.2.2 Isotopic fractionation

To validate the conservation of isotopic signatures, a N_2O reference gas (90.8 ppm N_2O) analysed by IRMS ($\delta^{15}N^\alpha = 25.9\pm0.4$‰ and $\delta^{15}N^\beta=25.2\pm1.0$‰) was diluted using high-purity synthetic air prior to preconcentration, followed by Tedlar bag sampling and QCLAS analysis (Table 1). Ambient (350 ppb), intermediate (900 ppb) and process (9.0 ppm) N_2O mixing ratios were supplied to the preconcentration unit. The standard preconcentration procedure was applied with an adsorption flow rate of 500 sccm during 20 min and 50 sccm (60–150 s) desorption flow. At elevated N_2O input mixing ratios (9.0 ppm) the desorbed sample gas was dynamically diluted by 1:10 during desorption by a fed-in flow, resulting in mixing ratios of ≈60 ppm for all experiments. A series (n=5–70) of preconcentration cycles were pooled in one Tedlar bag to obtain a gas sample of 3 to 5 l. Experiments at each mixing ratio level were replicated three to five times.

The N_2O isotopic composition of these samples after preconcentration was compared to the same reference gas diluted with synthetic air to a comparable N_2O mixing ratio (±1 ppm) to calculate $\Delta\delta^{15}N=\delta^{15}N_{precon}-\delta^{15}N_{original}$ (n=4–8). QCLAS calibration was performed using medical grade N_2O (91.1 ppm N_2O, $\delta^{15}N^\alpha=2.1\pm0.1$‰ and $\delta^{15}N^\beta=2.0\pm0.4$‰) and a gravimetrically prepared enriched gas (90.8 ppm N_2O, $\delta^{15}N^\alpha=25.9\pm0.4$‰ and $\delta^{15}N^\beta=25.2\pm1.0$‰) both analysed by IRMS (Toyoda and Yoshida, 1999).

2.2.3 Spectral interference

To evaluate potential spectral interferences from ambient air, samples were taken through a 5 m, 6 mm outer diameter PTFE tube from outside the laboratory building. The corresponding trace gas mixing ratios were taken from the routine measurements at the ≈300 m distant station Dübendorf of the Swiss National Air Pollution Monitoring Network (NABEL). Where no NABEL data were available (N_2O and CO_2), we assumed typical ambient mixing ratios as shown in Table 1. The standard preconcentration procedure (Sect. 2.1.1) was followed, and the desorbed gaseous species were analyzed either continuously (O_3, N_2O, CO_2, H_2O, CH_4, CO) or after Tedlar bag sampling (C_2H_2, O_2). Continuous data after preconcentration were obtained by FTIR (Sect. 2.1.2) for N_2O, CO_2, H_2O, CH_4, and CO. Ozone was measured using an UV absorption O_3 analyzer (TEI 49C, Thermo Fisher Scientific Inc., USA) after dynamic dilution with synthetic air. Oxygen was determined with an O_2 analyzer (Servomex 570A, Spectris plc, UK), and acetylene mixing ratios were obtained using a GC-FID (Agilent 6890 with Plot Al_2O_3 (KCl) column) after preconcentration with a Peltier cooled HayeSep D trap. The mixing ratios and corresponding preconcentration factors were then used to simulate absorption spectra and evaluate possible spectral interferences.
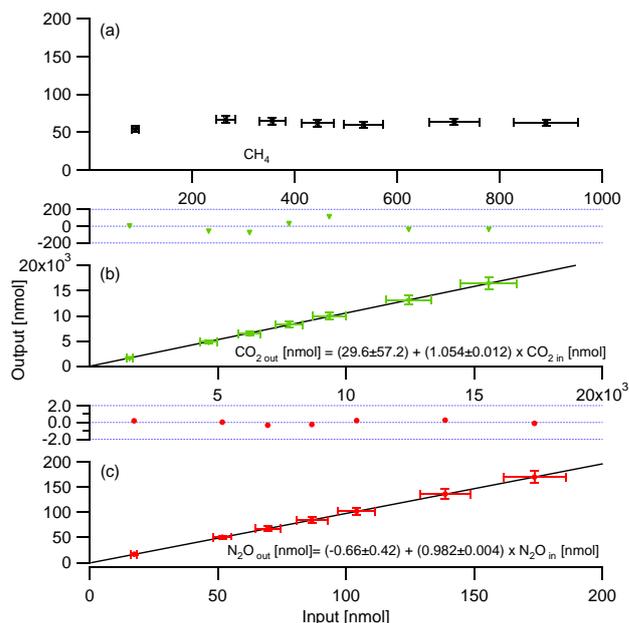
Fig. 4. Amount of **(a)** CH_4, **(b)** CO_2, and **(c)** N_2O concentrated on the HayeSep D trap depending on the sample volume from 1 to 10 l (adsorption: 100 sccm of 390 ppb N_2O, 35 ppm CO_2, 2.0 ppm CH_4, 350 ppb CO, 25 ppm H_2O in 80% N_2 and 20% O_2). Error bars represent the expanded standard uncertainty. For CO_2 and N_2O deviations from linearity are given in nmol.

3 Results and discussion

3.1 Trace gas recovery

Quantitative recovery of the adsorbed trace gases is a prerequisite to assure the representativeness of the analyzed gas sample and to avoid fractionation effects. Two different approaches were chosen to tackle this subject: (i) determination of the trace gas recovery with increasing adsorption volume to examine the trap capacity (Fig. 4); (ii) high-precision recovery of N_2O at different levels of mixing ratios (Table 2).

The capacity of the adsorbent trap for different trace gases was evaluated based on a sequence of experiments where 1 to 10 l of a gas mixture with constant composition (see Table 1) were first adsorbed on the preconcentration trap and then desorbed with a flow of 50 sccm of synthetic air and analyzed by on-line FTIR spectroscopy. For every trace gas the molar amounts in the input and output gas volume were calculated, integrating over time the respective mixing ratios and gas flows. The CO mixing ratio in the output flow was below the FTIR detection limit of 200 ppb and the amount of desorbed CH_4 was nearly constant and did not depend on gas sample volume (Fig. 4). This indicates that the mild adsorbent HayeSep D does not quantitatively retain CH_4 and CO at a trap temperature of approx. -150 °C which is above their respective boiling points of -161 °C and -191.5 °C.

For high precision N_2O isotopic analysis by QCLAS the loss of CO is an advantage because of its absorption in the selected spectral region. The application of the preconcentration unit for CO and CH_4 may still be envisaged by employing a stronger adsorbent (i.e. Molsieve 5Å) or an alternative refrigerant reaching a lower adsorption temperature.

As shown in Fig. 4, for N_2O and CO_2 a linear relation in the molar amounts between the trap output and the sample volumes was obtained, with expanded standard uncertainties for the regression lines of less than 1%. The linearity holds for the full investigated range, while the slight deviation from unity of 2% to 6%, is well below the uncertainty due to potential systematic offsets in the analysis of input and output mixing ratios by FTIR or in the input and output gas flows.

The efficiency of N_2O recovery is critical, because the adsorption/desorption processes may lead to significant isotopic fractionation (Bertolini et al., 2005; Brand, 1995; Werner et al., 2001). Therefore, a second, more precise approach was applied which allows the direct comparison of the sample gas before and after preconcentration by precise QCLAS measurements (Sect. 2.2.1). Using this experimental setup, the input and output mixing ratios agreed within 0.2% at ambient (350 ppb), intermediate (900 ppb) and process levels (9.0 ppm) (Table 2). Apart from the standard deviation for repetitive measurements, systematic deviations from e.g. subtle differences between the adsorbed and desorbed gas volumes cannot be excluded. However, such effects are considerably smaller than 1%, corresponding to a >99% recovery and thus, we expect only minimal, if any, isotopic fractionation.

3.2 Isotopic fractionation

To further confirm the conservation of isotopic signatures the isotopic composition of samples at ambient (350 ppb), intermediate (900 ppb) or process mixing ratios (9 ppm) were compared before and after preconcentration as described in Sect. 2.2.2. All experiments were done with gases that were enriched in $\delta^{15}N^\alpha$ by 25.9±0.4‰ and $\delta^{15}N^\beta$ by 25.2±1.0‰.

Agreement of the N_2O isotopic composition with/without preconcentration was in general very good (see Table 3). The $\delta^{15}N^\alpha$ values of N_2O after preconcentration are within 0.1‰ compared to the unprocessed calibration gas. For $\delta^{15}N^\beta$, the data seems to indicate a slight increase in the values after preconcentration, particularly at lower N_2O input mixing ratios. The uncertainty of the mean values is however rather large, and in a one-sided student's t-test the effect is not significant at the 0.05 significance level. We, nevertheless, plan to repeat the experiments in the future with the next generation of QCLAS and a directly coupled preconcentration unit. It should also be noted that the calibration routine will include the preconcentration step and can thus be expected to largely account for small fractionation effects if they really occur.

Table 2. High-precision recovery of N_2O after preconcentration ($n=3$). Error bars represent the expanded uncertainty (95% confidence level).

N_2O input mixing ratio	Recovery [%]
350 ppb	100.1±0.1
900 ppb	100.2±0.4
9.0 ppm	100.0±0.1

Table 3. Changes in the N_2O δ values ($\Delta\delta^{15}N=\delta^{15}N_{precon}-\delta^{15}N_{original}$) after dilution and preconcentration compared to the unprocessed calibration gas ($n=3-5$). Error bars represent the expanded uncertainty (95% confidence level).

N_2O input mixing ratio	$\Delta\delta^{15}N^\alpha$ [‰]	$\Delta\delta^{15}N^\beta$ [‰]
350 ppb	0.06±0.31	0.34±0.52
900 ppb	0.08±0.42	0.19±0.40
9.0 ppm	−0.05±0.38	0.07±0.80

3.3 Spectral interference

At the precision levels needed for N_2O isotope ratio analysis, even very weak spectral interferences of other compounds may be detrimental. To analyze spectral interferences of ambient air constituents the following approach was applied: (i) identification of molecular species (based on HITRAN database) that may cause spectral interferences through their absorption features; (ii) quantitative analysis of these components after preconcentration of ambient air, and (iii) assessment of spectral interferences based on spectral simulations.

Although the chosen absorption lines are free of any strong or obvious interference, we have considered all molecules in the HITRAN database (Rothman et al., 2005) for lines in the relevant wavelength region. The line strengths of the relevant molecules are plotted in Fig. 5b, weighted for their ambient molecular abundance (Table 1). Based on this abundance weighted representation, the most relevant interfering compounds are H_2O and CO_2, followed by CO, O_3 and C_2H_2. Apart from its spectral interference, the water content in the measuring gas has to be reduced considerably to avoid clogging of the adsorption trap. This is accomplished by permeation drying and $Mg(ClO_4)_2$, while CO_2 is largely removed by the Ascarite trap. For the other gas compounds, the preconcentration procedure is quite selective, as will be shown below.

Mixing ratios of H_2O and CO_2 were efficiently reduced during preconcentration, below their FTIR detection limits of 10 and 1 ppm, respectively. Both H_2O and CO_2 were shown to be efficiently removed by chemical trapping with

of the original "Medusa" for GC-MS. Wilhelm Gutjahr helped to conduct the numerous experiments needed to optimize the experimental conditions. Davide Ferri provided the FTIR gas cell, and Erwin Pieper and Willy Knecht contributed with their competence in mechanical design and electronics.

Edited by: F. Keppler

References

Bernard, S., Röckmann, T., Kaiser, J., Barnola, J.-M., Fischer, H., Blunier, T., and Chappellaz, J.: Constraints on N_2O budget changes since pre-industrial time from new firn air and ice core isotope measurements, Atmos. Chem. Phys., 6, 493–503, 2006, http://www.atmos-chem-phys.net/6/493/2006/.

Bertolini, T., Rubino, M., Lubritto, C., D'Onofrio, A., Marzaioli, F., Passariello, I., and Terrasi, F.: Optimized sample preparation for isotopic analyses of CO_2 in air: Systematic study of precision and accuracy dependence on driving variables during CO_2 purification process, J. Mass Spectrom., 40, 1104–1108, doi:10.1002/jms.888, 2005.

Billings, S. A.: Biogeochemistry: Nitrous oxide in flux, Nature, 456, 888–889, doi:10.1038/456888a, 2008.

Brand, W. A.: PRECON: A fully automated interface for the pre-GC concentration of trace gases in air for isotopic analysis, Isot. Environ. Health Stud., 31, 277–284, doi:10.1080/10256019508036271, 1995.

Brenninkmeijer, C. A. M. and Röckmann, T.: Mass spectrometry of the intramolecular nitrogen isotope distribution of environmental nitrous oxide using fragment-ion analysis, Rapid Commun. Mass Spectrom., 13, 2028–2033, doi:0951–4198/99/202028–06, 1999.

Brenninkmeijer, C. A. M., Janssen, C., Kaiser, J., Röckmann, T., Rhee, T. S., and Assonov, S. S.: Isotope effects in the chemistry of atmospheric trace compounds, Chem. Rev., 103, 5125–5161, doi:10.1021/cr020644k, 2003.

Faist, J., Capasso, F., Sivco, D. L., Sirtori, C., Hutchinson, A. L., and Cho, A. Y.: Quantum Cascade Laser, Science, 264, 553–556, doi:10.1126/science.264.5158.553, 1994.

FOEN and EMPA: Luftbelastung 2008, Messresultate des Nationalen Beobachtungsnetzes für Luftfremdstoffe (NABEL), Bern, 139 pp., 2009.

Gagliardi, G., Borri, S., Tamassia, F., Capasso, F., Gmachl, C., Sivco, D. L., Baillargeon, J. N., Hutchinson, A. L., and Cho, A. Y.: A frequency-modulated quantum-cascade laser for spectroscopy of CH_4 and N_2O isotopomers, Isot. Environ. Health Stud., 41, 313–321, doi:10.1080/10256010500384572, 2005.

Ishijima, K., Sugawara, S., Kawamura, K., Hashida, G., Morimoto, S., Murayama, S., Aoki, S., and Nakazawa, T.: Temporal variations of the atmospheric nitrous oxide concentration and its $\delta^{15}N$ and $\delta^{18}O$ for the latter half of the 20th century reconstructed from firn air analyses, J. Geophys. Res., 112, D03305, doi:10.1029/2006JD007208, 2007.

Kaiser, J., Röckmann, T., and Brenninkmeijer, C. A. M.: Complete and accurate mass spectrometric isotope analysis of tropospheric nitrous oxide, J. Geophys. Res., 108, D15, 4476, doi:10.1029/2003JD003613, 2003.

Kaiser, J., Engel, A., Borchers, R., and Röckmann, T.: Probing stratospheric transport and chemistry with new balloon and air-craft observations of the meridional and vertical N_2O isotope distribution, Atmos. Chem. Phys., 6, 3535–3556, 2006, http://www.atmos-chem-phys.net/6/3535/2006/.

Miller, B. R., Weiss, R. F., Salameh, P. K., Tanhua, T., Greally, B. R., Mühle, J., and Simmonds, P. G.: Medusa: A sample preconcentration and GC/MS detector system for in situ measurements of atmospheric trace halocarbons, hydrocarbons, and sulfur compounds, Anal. Chem., 80, 1536–1545, doi:10.1021/ac702084k, 2008.

Mohn, J., Forss, A. M., Brühlmann, S., Zeyer, K., Lüscher, R., Emmenegger, L., Novak, P., and Heeb, N.: Time-resolved ammonia measurement in vehicle exhaust, Int. J. Environ. Pollut., 22, 342–356, doi:10.1504/IJEP.2004.005548, 2004.

Mohn, J., Werner, R. A., Buchmann, B., and Emmenegger, L.: High-precision $\delta^{13}C$-CO_2 analysis by FTIR spectroscopy using a novel calibration strategy, J. Mol. Struct., 834, 95–101, doi:10.1016/j.molstruc.2006.09.024, 2007.

Mohn, J., Zeeman, M. J., Werner, R. A., Eugster, W., and Emmenegger, L.: Continuous field measurements of $\delta^{13}C$-CO_2 and trace gases by FTIR spectroscopy, Isot. Environ. Health Stud., 44, 241–251, doi:10.1080/10256010802309731, 2008.

Nakayama, T., Fukuda, H., Kamikawa, T., Sugita, A., Kawasaki, M., Morino, I., and Inoue, G.: Measurements of the $3\nu_3$ band of $^{14}N^{15}N^{16}O$ and $^{15}N^{14}N^{16}O$ using continuous-wave cavity ring-down spectroscopy, Appl. Phys. B, 88, 137–140, doi:10.1007/s00340-007-2653-3, 2007.

Nelson, D. D., McManus, J. B., Herndon, S. C., Zahniser, M. S., Tuzson, B., and Emmenegger, L.: New method for isotopic ratio measurements of atmospheric carbon dioxide using a 4.3 μm pulsed quantum cascade laser, Appl. Phys. B, 90, 301–309, doi:10.1007/s00340-007-2894-1, 2008.

Park, S., Atlas, E. L., and Boering, K. A.: Measurements of N_2O isotopologues in the stratosphere: Influence of transport on the apparent enrichment factors and the isotopologue fluxes to the troposphere, J. Geophys. Res., 109, D01305, doi:10.1029/2003JD003731, 2004.

Rahn, T. and Wahlen, M.: A reassessment of the global isotopic budget of atmospheric nitrous oxide, Glob. Biogeochem. Cycle, 14, 537–543, doi:0886-6236/00/1999GB 900070, 2000.

Ravishankara, A. R., Daniel, J. S., and Portmann, R. W.: Nitrous oxide (N_2O): The dominant ozone-depleting substance emitted in the 21st century, Science, 326, 123–125, doi:10.1126/science.1176985, 2009.

Röckmann, T., Kaiser, J., and Brenninkmeijer, C. A. M.: The isotopic fingerprint of the pre-industrial and the anthropogenic N2O source, Atmos. Chem. Phys., 3, 315–323, 2003, http://www.atmos-chem-phys.net/3/315/2003/.

Röckmann, T. and Levin, I.: High-precision determination of the changing isotopic composition of atmospheric N_2O from 1990 to 2002, J. Geophys. Res., 110, D21304, doi:10.1029/2005JD006066, 2005.

Rothman, L. S., Jacquemart, D., Barbe, A., Benner, D. C., Birk, M., Brown, L. R., Carleer, M. R., Chackerian, C., Chance, K., Coudert, L. H., Dana, V., Devi, V., M., Flaud, J. M., Gamache, R. R., Goldman, A., Hartmann, J. M., Jucks, K. W., Maki, A. G., Mandin, J. Y., Massie, S. T., Orphal, J., Perrin, A., Rinsland, C. P., Smith, M. A. H., Tennyson, J., Tolchenov, R. N., Toth, R. A., Vander Auwera, J., Varanasi, P., and Wagner, G.: The HITRAN 2004 molecular spectroscopic database, J. Quant. Spectrosc.

Radiat. Transf., 96, 139–204, doi:10.1016/j.jqsrt.2004.10.008, 2005.

Solomon, S., Qin, D., Manning, M., Chen, Z., Marquis, M., Averyt, K. B., Tignor, M., and Miller, H. L.: IPCC, 2007: Climate Change 2007: The Physical Science Basis, Cambridge Univ. Press, Cambridge and New York, 987 pp., 2007.

Toyoda, S., and Yoshida, N.: Determination of nitrogen isotopomers of nitrous oxide on a modified isotope ratio mass spectrometer, Anal. Chem., 71, 4711–4718, doi:10.1021/ac9904563, 1999.

Toyoda, S., Yoshida, N., Urabe, T., Aoki, S., Nakazawa, T., Sugawara, S., and Honda, H.: Fractionation of N$_2$O isotopomers in the stratosphere, J. Geophys. Res., 106, 7515–7522, 2001.

Toyoda, S., Yoshida, N., Urabe, T., Nakayama, Y., Suzuki, T., Tsuji, K., Shibuya, K., Aoki, S., Nakazawa, T., Ishidoya, S., Ishijima, K., Sugawara, S., Machida, T., Hashida, G., Morimoto, S., and Honda, H.: Temporal and latitudinal distributions of stratospheric N$_2$O isotopomers, J. Geophys. Res., 109, D08308, doi:10.1029/2003JD004316, 2004.

Toyoda, S., Iwai, H., Koba, K., and Yoshida, N.: Isotopomeric analysis of N$_2$O dissolved in a river in the Tokyo metropolitan area, Rapid Commun. Mass Spectrom., 23, 809–821, doi:10.1002/rcm.3945, 2009.

Tuzson, B., Mohn, J., Zeeman, M. J., Werner, R. A., Eugster, W., Zahniser, M. S., Nelson, D. D., McManus, J. B., and Emmenegger, L.: High precision and continuous field measurements of δ^{13}C and δ^{18}O in carbon dioxide with a cryogen-free QCLAS, Appl. Phys. B, 92, 451–458, doi:10.1007/s00340-008-3085-4, 2008a.

Tuzson, B., Zeeman, M. J., Zahniser, M. S., and Emmenegger, L.: Quantum cascade laser based spectrometer for in situ stable carbon dioxide isotope measurements, Infrared Phys. Technol., 51, 198–206, doi:10.1016/j.infrared.2007.05.006, 2008b.

Uehara, K., Yamamoto, K., Kikugawa, T., and Yoshida, N.: Isotope analysis of environmental substances by a new laser-spectroscopic method utilizing different pathlengths, Sens. Actuators B, 74, 173–178, doi:10.1016/S0925-4005(00)00729-2, 2001.

Uehara, K., Yamamoto, K., Kikugawa, T., and Yoshida, N.: Site-selective nitrogen isotopic ratio measurement of nitrous oxide using 2 μm diode lasers, Spectrochim. Acta A, 59, 957–962, doi:10.1016/S1386-1425(02)00260-3, 2003.

VDI: 2449 Part 1 – Prüfkriterien von Meßverfahren – Ermittlung von Verfahrenskenngrößen für die Messung gasförmiger Schadstoffe (Immission), Düsseldorf, 45 pp., 1995.

Wächter, H. and Sigrist, M. W.: Mid-infrared laser spectroscopic determination of isotope ratios of N$_2$O at trace levels using wavelength modulation and balanced path length detection, Appl. Phys. B, 87, 539–546, doi:10.1007/s00340-007-2576-z, 2007.

Wächter, H., Mohn, J., Tuzson, B., Emmenegger, L., and Sigrist, M. W.: Determination of N$_2$O isotopomers with quantum cascade laser based absorption spectroscopy, Opt. Express, 16, 9239–9244, doi:10.1364/OE.16.009239, 2008.

Well, R., Flessa, H., Xing, L., Xiaotang, J., and Römheld, V.: Isotopologue ratios of N$_2$O emitted from microcosms with NH$_4^+$ fertilized arable soils under conditions favoring nitrification, Soil Biol. Biochem., 40, 2416–2426, doi:10.1016/j.soilbio.2008.06.003, 2008.

Werle, P., Mucke, R., and Slemr, F.: The limits of signal averaging in atmospheric trace-gas monitoring by tunable diode-laser absorption-spectroscopy (TDLAS), Appl. Phys. B, 57, 131–139, doi:10.1007/BF00425997, 1993.

Werner, R. A. and Brand, W. A.: Referencing strategies and techniques in stable isotope ratio analysis, Rapid Commun. Mass Spectrom., 15, 501–519, doi:10.1002/rcm.258, 2001.

Werner, R. A., Rothe, M., and Brand, W. A.: Extraction of CO$_2$ from air samples for isotopic analysis and limits to ultra high precision δ^{18}O determination in CO$_2$ gas, Rapid Commun. Mass Spectrom., 15, 2152–2167, doi:10.1002/rcm.487, 2001.

Yoshida, N. and Toyoda, S.: Constraining the atmospheric N$_2$O budget from intramolecular site preference in N$_2$O isotopomers, Nature, 405, 330–334, doi:10.1038/35012558, 2000.